

Claisen thermally rearranged (CTR) polymers

Alberto Tena,^{1*} Sofia Rangou,¹ Sergey Shishatskiy,¹ Volkan Filiz,¹ Volker Abetz^{1,2}

2016 © The Authors, some rights reserved; exclusive licensee American Association for the Advancement of Science. Distributed under a Creative Commons Attribution NonCommercial License 4.0 (CC BY-NC).
10.1126/sciadv.1501859

Thermally rearranged (TR) polymers, which are considered the next-generation of membrane materials because of their excellent transport properties and high thermal and chemical stability, are proven to have significant drawbacks because of the high temperature required for the rearrangement and low degree of conversion during this process. We demonstrate that using a [3,3]-sigmatropic rearrangement, the temperature required for the rearrangement of a solid glassy polymer was reduced by 200°C. Conversions of functionalized polyimide to polybenzoxazole of more than 97% were achieved. These highly mechanically stable polymers were almost five times more permeable and had more than two times higher degrees of conversion than the reference polymer treated under the same conditions. Properties of these second-generation TR polymers provide the possibility of preparing efficient polymer membranes in a form of, for example, thin-film composite membranes for various gas and liquid membrane separation applications.

INTRODUCTION

Internal interconnected microvoids of polymers determined as free volume result from chain mobility and substantial packing disorder of covalently bonded polymer chains. Lately, studies on high free-volume polymers, known as microporous organic polymers, have been published (1). High fractional free-volume (FFV) glassy polymers (for example, polymers of intrinsic microporosity) (2, 3) or thermally rearranged (TR) polymers (4) generally present large and well-interconnected free-volume elements that have characteristic diameters in the range of 4 to 9 Å (5). Because of their easy synthesis and fabrication, these highly permeable polymers are favorable candidates for large-scale industrial membrane separation processes (for example, carbon dioxide capture and storage, industrial nitrogen generation, ammonia production, processing of gaseous refinery streams, and natural gas sweetening), which have the potential of minimizing process complexity and reducing energy consumption.

TR polymers with high permeability and superior physical properties are a novel class of polymers prepared by a two-step synthetic process, in which aromatic polyimides or polyamides with *ortho*-functional groups are thermally rearranged into heteroaromatic polymers (PB-X) [for example, polybenzoxazole (PBO), polybenzothiazole, polypyrrolone, and polybenzimidazole]. The temperature required for a complete conversion varies with the structure (6), but, usually, it is close to 450°C (7). During the structural rearrangement of polymers in the solid state, the distortion of the polyimide chain into a rigid-rod polymer leads to the formation of two different types of microcavities with diameters in the range of 3 to 4 Å and 7 to 9 Å (8), where the smaller-sized microcavities could be beneficial for the selective transport of different molecules and the larger pores for the diffusion. The microporosity (free-volume element size and distribution) of the TR polymers is controlled by the fabrication conditions in terms of treatment time and temperature, in contrast to commonly used microporous materials. Moderate selectivities while maintaining high permeabilities within the interconnected free-volume elements enable exceeding the trade-off relationships for industrially relevant gas pairs such as O₂/N₂, CO₂/N₂, or CO₂/CH₄ (9) and exhibit excellent properties for other applications in gas/liquid separations, liquid/liquid separations (10, 11), or ion-conductive batteries (12). Because of their free-volume

void size distribution and thermal and hydrothermal stability, the use of these polymers can be broadened to applications where other materials like, for example, zeolites are already used [microelectronics (13), catalysis (14), or medical diagnosis (15)].

Despite the prospect of using TR polymers for high-performance membranes in gas separation processes, the high temperatures required to complete the rearrangement remain a major factor limiting the polymers' practical application. The applicability of TR polymers can be significantly advanced by reducing the conversion temperature to a more energy-efficient level and by using commercially available monomers (16). Lowering the processing temperature will result in a significant reduction of the polymer chain degradation, which occurs during the rearrangement at high temperatures; minimization of the effect of other uncontrollable reactions that lead to a drastic decrease of the mechanical properties of the material.

Guo *et al.* investigated polyimides with more flexible macromolecular chains and, subsequently, lower glass transition temperature (T_g), which led to a reduction of the rearrangement temperature by 100°C (from 450° to 350°C) for a total conversion to PBO. However, the flexibility of the polymer chains led to a drastic negative effect on the final gas transport properties of the polymer (17).

PB-X structures could be obtained from *ortho*-X polyamide derivatives (PA) as well. For example, the comparison between *ortho*-hydroxy polyamides (HPA) and *ortho*-hydroxy polyimide (HPI) reveals that the HPA structures require lower temperatures to undergo the thermal rearrangement into the corresponding PBO (18). This is possibly due to the greater flexibility around the aromatic amide linkage of the hydroxyl groups in PHA compared to that of the tertiary amine in HPI. Thus, PHAs can be thermally rearranged at temperatures usually 100°C lower than that of HPIs. Despite this, the effect on the separation properties is marked, causing the permeability coefficients to drop below any values suitable for practical membrane application. Therefore, new methods leading to a reduction of the rearrangement temperature should be developed. This will enable a promising future for these materials as separation membranes.

A change in the rearrangement mechanism is key to reducing the energy required for the process to take place. Despite this mechanism not being completely clear, it is generally accepted that the first step of the rearrangement is the reaction of the *ortho*-functional groups (–OH, –NH₂, or –SH) with the carbon (electrophilic) of the carbonyl group present in the polyimide.

¹Institute of Polymer Research, Helmholtz-Zentrum Geesthacht, Max-Planck-Str.1, 21502 Geesthacht, Germany. ²Institute of Physical Chemistry, University of Hamburg, Martin-Luther-King-Platz 6, 20146 Hamburg, Germany.

*Corresponding author. Email: alberto.tena@hzg.de

In 1912, Claisen (19) reported a thermal isomerization of an allyl vinyl ether (or nitrogen or sulfur containing analog derivatives) leading to a bifunctionalized molecule in a $[\pi^2s + \sigma^2s + \pi^2s]$ process. The reaction can take place in the same way in an aromatic compound, as represented in Fig. 1 (20). For Claisen rearrangement in allyl phenyl ethers, the first [3,3]-sigmatropic rearrangement step results in an *ortho*-dienone, which usually quickly tautomerizes to an *ortho*-substituted phenol. This reaction is known as the *ortho*-Claisen rearrangement, and it can take place between 160° and 250°C, depending on the reaction conditions (for example, solvent and pressure) and the character and position of the substituents (21).

Ortho-Claisen rearrangement has not been described for polymers until now. In the case of polyimides or polyamides with *ortho*-functional groups, similar conditions to those of smaller molecules can be met, and then, the reaction can take place. The reaction has also not been described in the solid state because it would be hindered because of the dense state of the polymer. Obviously, once there is no solvent in the medium, the conditions of the reaction initiation should be different, resulting in, for example, higher temperatures or lower yields, but there is no reason not to expect the same mechanism to occur. Thus, it is possible to plan the same rearrangement process in a polymer, and, more specifically, in the case of *ortho*-X polyimides and polyamides, enabling them to undergo a thermal rearrangement.

Here, a new method of functionalization of the *ortho*-hydroxyl groups of the polyimide is studied. The method for obtaining the corresponding polyimide with an allyl ether group in *ortho*-position of the imide ring is described. The obtained polymer, being in the solid state,

is subjected to the Claisen rearrangement during the heat treatment, which is at least 100°C lower than that necessary for the classical thermal rearrangement, yielding the corresponding poly(*o*-hydroxyimide) as a product. The reaction further evolves to the corresponding PBO, resulting in a polymer with very attractive gas transport properties and good mechanical properties.

RESULTS AND DISCUSSION

Classical TR precursor polyimide polymers were synthesized by polycondensation reaction, followed by azeotropic imidization. Afterward, by simple postmodification of the polymers, allylation of the hydroxyl group in *ortho*-position to the imide group was performed. Once the film of a corresponding polymer was formed, the characterization of polymer properties was carried out.

In Fig. 2, the thermal behavior of the pristine, in comparison to the functionalized polymers derived from 6FDA-HAB, is depicted. Two steps of weight loss can be distinguished for pristine and allyl-functionalized polymers: an initial mass loss occurring at 260° to 370°C for allyl-functionalized polymers and 320° to 475°C for the pristine polymer, and a second weight loss common for both polymers, ranging from 475° to 550° to 800°C. The first mass loss is associated with the rearrangement reaction. Using thermogravimetric analysis coupled with Fourier transform infrared spectroscopy (TGA/FTIR), it was demonstrated that only carbon dioxide leaves the polymer during the first weight loss step for both polymers. The weight change for this step was 12.5% for the allyl-functionalized

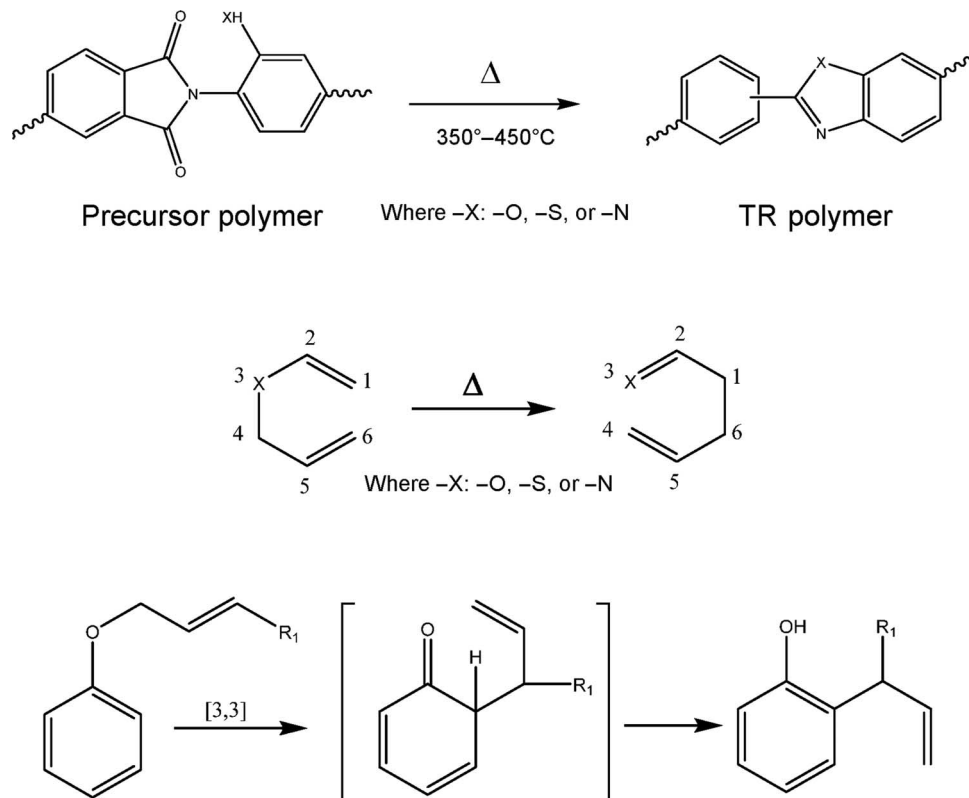


Fig. 1. General schemes of TR polymers, first description of the Claisen rearrangement, and aromatic Claisen rearrangement.

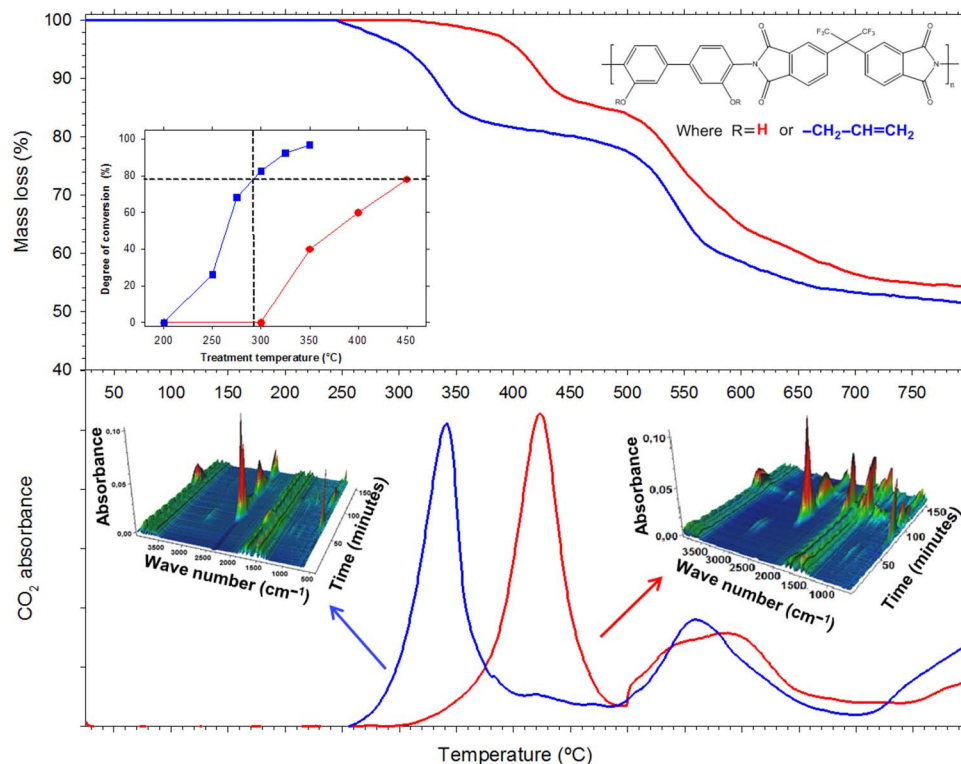


Fig. 2. Mass loss and absorbance spectra of CO₂ as a function of temperature for the pristine and allyl-functionalized 6FDA-HAB polymers.

polymer and 14.1% for the pristine polymer, which agrees with the theoretical weight loss of the polymer necessary for the full rearrangement from polyimide to PBO. The second step of weight loss was due to the thermal decomposition of the corresponding aromatic PBO, and it was similar in both cases.

An obvious difference in the rearrangement temperature of almost 100°C was observed for these two polymers, and, despite this big difference, no effect on thermal degradation was detected. This temperature difference of the rearrangement impacts polymer conversion as well. Whereas a conversion close to 80% was obtained for the pristine polymer at 450°C, the same degree of conversion can be reached at temperatures lower than 300°C for the functionalized polymer. The reduction of the temperature necessary for the rearrangement obviously leads to a large gap between rearrangement and degradation process temperatures (as observed in fig. S1). Whereas the pristine polymer rearrangement and degradation temperature ranges overlap, these temperatures are over 100°C apart for the allyl-functionalized polymer (see table S1). The degree of conversion to PBO as a function of the thermal treatment as well as the tridimensional IR spectrum recorded during the complete process at different times (related to temperature, heating rate was 5°C/min) are also depicted in Fig. 2. Obviously, because of the fact that the rearrangement temperature was reduced, materials with a much higher degree of conversion at much lower temperatures of thermal treatment were obtained. In this case, an almost complete conversion from polyimide to PBO for the allyl-functionalized polymer could be achieved at 350°C.

Fourier transform IR (FTIR) spectra (fig. S2) showed the evolution of the characteristic absorption bands of allyl-functionalized polymers at

different temperatures of treatment: the stretching vibration bands of C=O (1794 and 1726 cm⁻¹), asymmetric stretching of C-N (1380 cm⁻¹), and the transverse stretching of C-N-C groups at 1100 cm⁻¹ decreased with the thermal treatment, and new characteristic benzoxazole bands, for example, 1620 cm⁻¹ (stretching C=N) or 1060 cm⁻¹ (aromatic -O-C stretching), appeared. Absorption peaks of C-F stretching at around 1250 to 1100 cm⁻¹ were confirmed to be intact after the different thermal treatments. No peaks were observed in the region of 3200 to 3600 cm⁻¹ attributed to the O-H vibration of the hydroxyl groups. Small differences in the stretching and bending modes in aromatic regions (1600 to 1550 cm⁻¹ and 950 to 700 cm⁻¹), respectively, were observed. Unfortunately, the presence of allyl groups could not be confirmed by FTIR. Comparison between pristine and functionalized polymers after the corresponding thermal treatments did not show significant differences (fig. S3), which confirms that pristine and allyl-functionalized polymers have a similar final structure.

The differential scanning calorimetry (DSC) study indicated that, in both cases, the rearrangement takes place at temperatures close to the T_g . For the pristine polymer, the rearrangement starts at temperatures close to the T_g of the polymer (330°C), whereas for the allyl-functionalized polymer, the process starts parallel with the Claisen rearrangement at a temperature lower than the T_g (280°C). It is clear that the chain rigidity of the initial polymer influences the temperature of thermal conversion to PBO. The difference in the T_g between pristine and functionalized polymers is smaller than that in the temperature necessary for the start of thermal rearrangement. These differences are especially important in the maximum rearrangement reaction rates (approximately 80°C) and the end of the rearrangement (approximately 100°C). Thus, it

can be proposed that higher mobility of the polymer chain and further activation of the oxygen in the *ortho*-position of the imide after the Claisen rearrangement favors the process.

Given this information, it could be hypothesized that the mechanism of Claisen TR (CTR) polymer rearrangement to PBO has at least two different steps, as represented in Fig. 3. The first step is the Claisen rearrangement, immediately followed by the second step, in which the negatively charged oxygen atom in the *ortho*-position of the imide group reacts with the positive carbon of the carbonyl group. In the second step, the corresponding polyimide undergoes the transformation into PBO, as represented in Fig. 2, and followed by ^1H - and ^{13}C -nuclear magnetic resonance (NMR) (fig. S4 to S6).

The NMR study gave a clear indication of how both rearrangements occur. At around 80 ppm, the representative signal for the $-\text{O}-\text{CH}_2-$ bond was identified. This signal is completely shifted to around 30 ppm for the sample treated at 350°C , an indication that the Claisen rearrangement has been performed. The same was observed for the peak at 112 ppm. This peak is an indication on how the signal for aromatic carbon close to the allyl ether (peak number 4 in the fig. S6) changes until complete disappearance. The existence of allyl groups in the final structure was confirmed by the peak at 117 ppm. The thermal rearrangement in the polymer is confirmed by the disappearance of the typical peak for carbonyl (peak number 1 in the fig. S6) and the appearance of the typical peak for oxazole structures (peak number 7 in the fig. S6) in the same way as described by Smith *et al.* (18).

Additional reactions can occur between the allyl units [for example, cross-linking (22) or aromatization (23)]. For this reason, some allyl groups could not be present in the final structure. Intermolecular reactions could result in insoluble polymers because of cross-linking reactions (24) as well. A high degree of cross-linking in the final structure was confirmed by gel content determination. A Soxhlet extractor was used to determine the gel fraction of the CTR polymer treated at 350°C . In this case, two different solvents, tetrahydrofuran and dimethyl sulfoxide (DMSO), were selected. The sample was refluxed in the extractor for approximately 24 hours and then dried at 200°C for another 24 hours,

yielding 0 and 0.5% of loss mass, respectively, which leads to the conclusion that the CTR samples were intensively cross-linked.

Despite the big decrease in the rearrangement temperature for the CTR polymer, the degradation temperature was similar for both polymers. For this reason, a great improvement in the mechanical robustness of the polymeric films is observed with respect to the reported brittleness of the classical TR polymers (25). The inclusion of the aliphatic substituent in the *ortho*-position of the polyimide leads to an increase in the flexibility of the polymer chain and a reduction in the interactions by hydrogen bonds, resulting in the mechanical robustness of the CTR polymer that allows severe film bending (Fig. 4) of the functionalized CTR polymer sample thermally treated at 350°C . This excellent behavior was confirmed by the mechanical properties study (table S2). CTR polymer thermally treated at 350°C showed values for the Young modulus similar to classical TR polymer thermally treated at 450°C but with higher maximum stress and significantly higher strain values. CTR and classical TR polymers showed similar values of Young modulus and strain when both polymers were thermally treated at 350°C . It confirms that higher temperatures of thermal treatment provoke overlapping effects of thermal rearrangement and polymer degradation, resulting in unacceptably low mechanical properties of classical TR polymers, which lead to substantial difficulties in use of these materials for membrane separation processes.

Kushwaha *et al.* recently demonstrated that a reduction of the rearrangement temperature to 350°C and lower, apart from resulting in more mechanically stable films, gives the opportunity to carry out the thermal treatment under air atmosphere (25). Thus, the advance of rearrangement temperature reduction through Claisen reaction will lead to an important improvement in the processing of the polymer, fostering a wide application of TR polymers in separation processes at harsh conditions where conventional polymers are losing their properties because of, for example, swelling or even degradation (26).

To prove the concept, the aforementioned functionalization route was followed for other polymers as well. For the CTR polymers discussed above, only the thermal properties were evaluated. The complete study was made for the 6FDA-HAB polymer to compare results to the

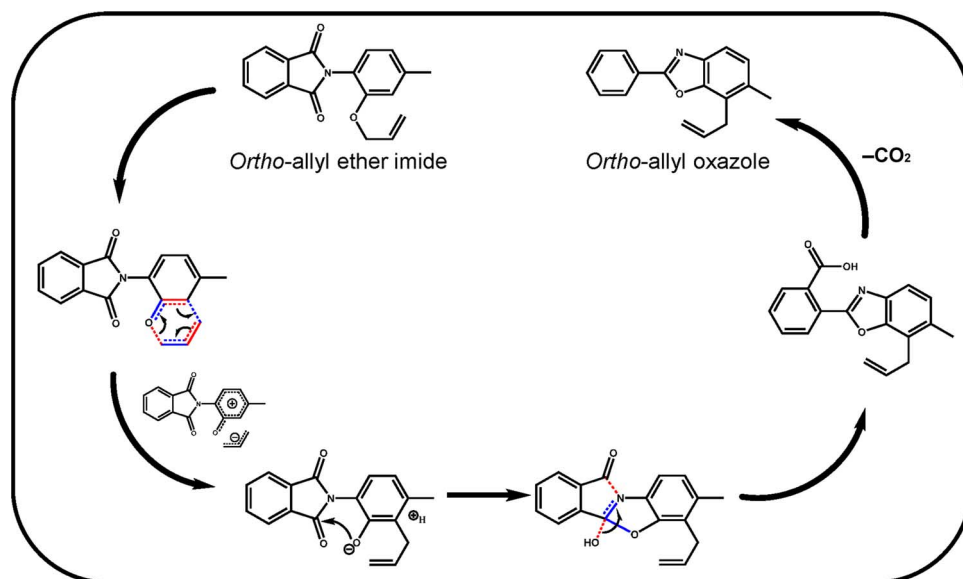


Fig. 3. Proposed mechanism. Claisen rearrangement is just the first step of the process.

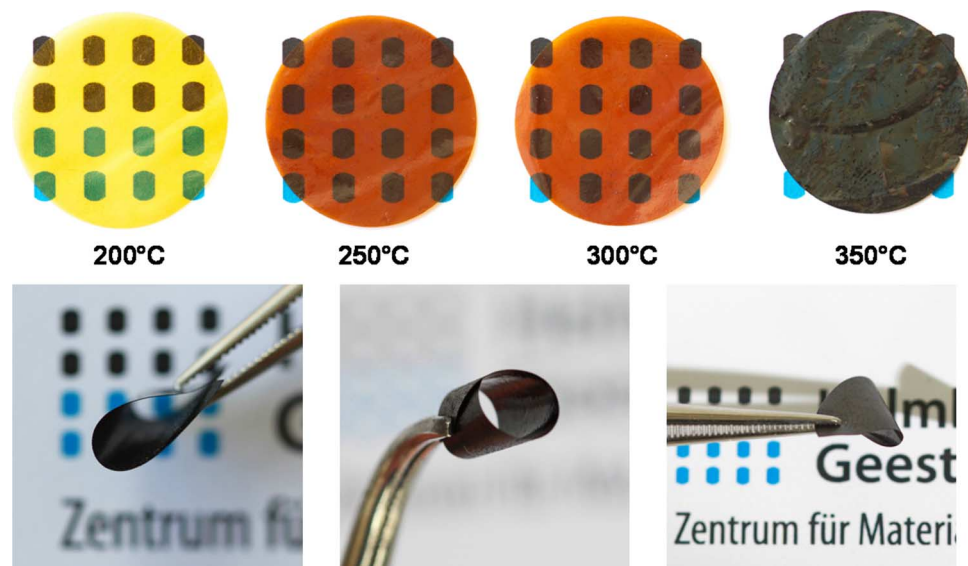


Fig. 4. Physical appearance and mechanical robustness for the CTR polymers.

existing numerous reports. In all cases (6FDA-BisAPAF, BTDA-BisAPAF, and PMDA-BisAPAF), a thermal behavior similar to that of the 6FDA-HAB polymer was found (fig. S7). The temperature for the rearrangement was reduced for all the allyl derivatives with respect to the pristine polymers. For the PMDA-BisAPAF-allyl polymer, the reduction was especially remarkable (see table S3). This polymer already reaches 50% conversion at 260°C. The temperature for a complete conversion of this polymer was slightly higher than 300°C, in contrast to the significantly higher temperatures necessary for the complete rearrangement of the pristine polymer (around 490°C). The reduction of almost 200°C in the rearrangement temperature for a complete conversion opens the way for even thin-film composite membrane production consisting solely of polymeric materials.

TR polymers are currently well known for their excellent gas separation properties. It has been demonstrated that, by a functionalization of the polymer chain, gas transport properties were strongly altered, leading to an insignificant decrease of the permeability but a great increase in the selectivity (27). Apart from the main achievement of this work, namely, the reduction of the rearrangement temperature of the TR polymers, gas transport properties were determined.

The effectiveness of the CTR process becomes obvious when one compares gas transport properties of the pristine and functionalized polymers treated at 350°C (Fig. 5). It was observed that CTR polymers were almost five times more permeable (see table S4) because of more than two times higher degree of conversion than the classical TR polymer treated under the same conditions (1 hour at 350°C), whereas ideal selectivities for various gas pairs were similar for both materials. This behavior is observed because, for the same thermal treatment, the degree of conversion under the same conditions (1 hour at 350°C) was about 98% for the CTR polymer compared to just 40% of conversion for the classical TR polymer, and no degradation was observed for the final PBO obtained from the CTR polymer. Therefore, it is important to achieve a high degree of conversion at a temperature below the onset of the chemical degradation.

The increase in permeability in both cases of CTR and classical TR polymers is derived from the increase in the FFV (table S5), resulting in

higher mobility of the penetrant molecules in the polymer matrix or increased diffusivity. CTR polymers were less permeable but more selective than the classical TR. This effect can be easily observed in the analysis of the solubility and diffusivity as a function of the percentage of conversion (fig. S8). For the CTR polymers, CO₂ solubility was higher and increased slightly with the temperature of the thermal treatment. The same effect was observed for the CO₂ diffusivity. In the case of the classical TR polymers, CO₂ solubility was lower than that for the CTR polymers and decreased with the temperature of the thermal treatment. On the other hand, CO₂ diffusivity was much higher and increased with the degree of conversion to PBO. Incorporation of allyl units into the polymer chain results in an increase of CO₂ solubility with respect to the pristine polymer. The degree of conversion to PBO influences the CO₂ solubility, which increases with increased degrees of conversion. The CO₂ diffusivity increased for both CTR and classical TR polymers, but the increase was much higher in the classical TR polymers. The effect was clearly observed for CO₂ (fig. S9A) but also can be observed for O₂ (see fig. S9B).

The properties of the polymers under study directly depend on the synthesis procedure (8). For this reason, only the polymers synthesized in the same way were selected for demonstration. A similar trend was found in the comparison of the pristine polymer synthesized and characterized in the current study and the polymers reported earlier. The reported pristine 6FDA-HAB polymer thermally treated at 450°C (17, 28, 29) has lower permeability and selectivity than 6FDA-HAB-allyl thermally treated at 350°C. It should be emphasized that the gas transport properties of the CTR polymer treated at 350°C for the CO₂/CH₄ gas pair are very close to the new 2008 Robeson's upper bound and are better compared with the properties of the classical TR polymers thermally treated at 450°C. The improvement in the gas transport properties of CTR polymers can be observed in Fig. 6 and fig. S9, where the results of the current study are compared to those reported earlier. Enhanced gas transport properties, accompanied by attractive mechanical properties, highlight the future of these polymers.

Reduction of the rearrangement temperature for CTR polymers compared to previously reported TR polymers results in a low level

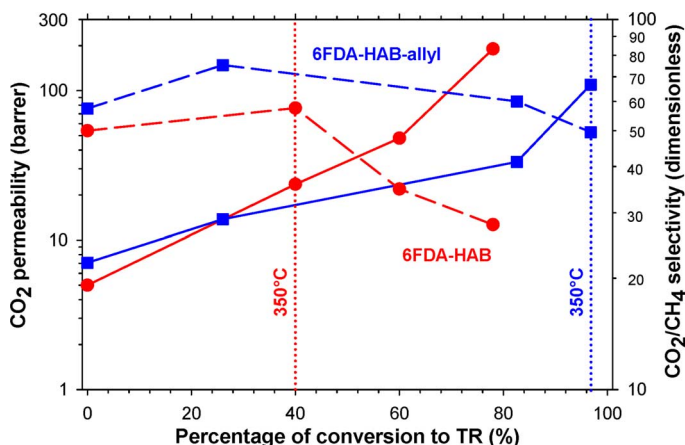


Fig. 5. Evaluation of the CO₂/CH₄ separation properties as a function of the degree of conversion. Continuous lines represent the evolution of the CO₂ permeability and dashed lines represent CO₂/CH₄ selectivity. Vertical dotted lines denote the results at the same treatment temperature for the CTR polymer (squares) and the classical TR polymer (circles).

of degradation of the polymer chains, lower permeabilities, and much higher selectivities. Absence of the chain decomposition, accompanied by high conversion to PBO (30), is beneficial for the diffusion of small molecules in the polymer, similar to carbon molecular sieve membranes (31). The generation of excessively high FFV in the polymer leads to decreased or low gas permselectivity. In the case of CTR polymers, the increase in the permeability is relatively low, but the selectivity remains high. The gas transport mechanism is similar to the case of carbon molecular sieves obtained from polymers (32). It was experimentally confirmed that the classical TR polymers have two types of pore sizes (or free-volume elements): ultramicropores, for free-volume void size lower than 6 Å, and micropores, for voids between 6 and 20 Å (32). In the case of the classical TR polymers, with the increase of the thermal treatment temperature, each polymer transforms from a low-permeable and highly selective material to a more permeable and less selective one. This is possible due to the increase in both average free-volume void size and their interconnection. For low treatment temperature, for example, at 350°C, a similar selectivity and an increased permeability of the materials were observed in comparison between the CTR polymer and the untreated pristine polymer. This can be only possible because the fraction of selective ultramicropores increases in the structure of the material without evolving them into highly interconnected bigger free-volume elements. Above this treatment temperature, there is an evolution in quantity and size of the micropores, resulting in higher free-volume void interconnection (33), contributing to the increase of the permeability and reduction of the selectivity (34). A similar effect was attributed to the thermal decomposition during the first stages of the carbonization of a commercial polyimide (35). According to the proposed approach, we were able to increase the permeability with FFV increase, but the number of “bottle necks” and their size were still low enough to keep the high diffusivity selectivity level of the material.

The CO₂ transport through CTR polymer was characterized at elevated feed pressures to analyze the polymer stability against plasticization caused by highly soluble penetrant (fig. S10). As expected, and well described in the literature (4), TR polymers showed excellent plasticization resistance at high CO₂ feed pressures. After the typical loss of

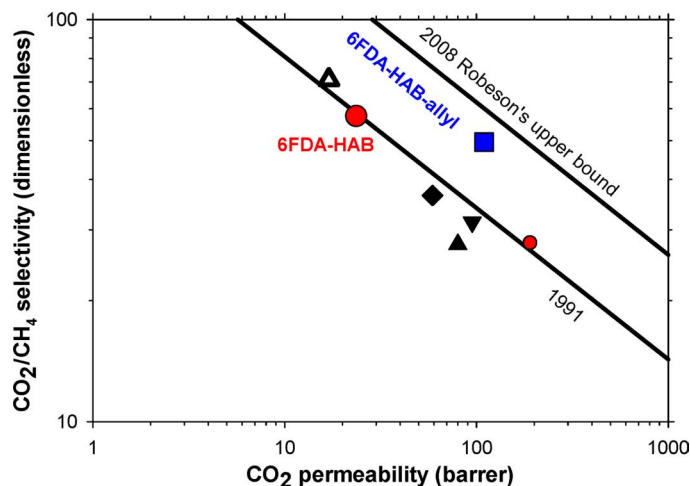


Fig. 6. Robeson's trade-off for the CO₂/CH₄ gas pair. Samples are represented by symbols as follows: circles for 6FDA-HAB; squares for 6FDA-HAB-allyl; and diamonds (17), triangles pointing down (29), and triangles pointing up (28) for literature data on the polymer 6FDA-HAB synthesized under the same conditions. The largest symbols are for samples thermally treated at 350°C, and small symbols are for the samples thermally treated at 450°C.

permeability at the low pressures, the permeability was kept constant up to 40 bar pressure. Real gas mixture transport properties of CTR polymer were also studied with the binary gas mixture containing 60% methane and 40% carbon dioxide at 25°C and 50 bar feed pressure. The same polymer sample was measured three times with depressurization between experiments to analyze stability of the sample and reproducibility of results. Membranes showed excellent plasticization resistance and exceptional CO₂/CH₄ selectivity (43.8 ± 1.4) for the studied binary mixture. As expected from previous reports (4), the mixed gas selectivity was slightly lower than the ideal one obtained from the pure gas experiments but still attractively high.

The developed new CTR polymers can be considered as a second generation of TR polymers having attractively high gas transport and mechanical properties. Different allyl derivatives could be introduced into the polymer chains to reduce the rearrangement temperature, improving the solubility of corresponding precursors in organic solvents suitable for membrane formation or mechanical properties of the final rearranged polymer. Consequently, a new line of polymers can be developed and applied for various membrane separation applications.

MATERIALS AND METHODS

Chemicals

The dianhydrides 4,4'-(hexafluoroisopropylidene)diphthalic anhydride (6FDA), 3,3',4,4'-biphenyltetracarboxylic dianhydride (BPDA), 3,3',4,4'-benzophenonetetracarboxylic acid dianhydride (BTDA), 1,2,4,5-benzene tetracarboxylic dianhydride (PMDA), and the diamines 3,3'-dihydroxy-4,4'-diamino-biphenyl (HAB) and 2,2'-bis(3-amino-4-hydroxyphenyl) hexafluoropropane (bisAPAF) were purchased from Sigma-Aldrich. Dianhydrides were purified by sublimation at high vacuum just before use. Diamines were dried at 120°C in vacuum for 12 hours and stored in a desiccator at vacuum until use.

Reactants and solvents, such as chlorotrimethyl silane, pyridine, acetic acid, *N,N*-dimethyl amino pyridine (DMAP), 3-bromopropene or allyl bromide, potassium carbonate (K_2CO_3), *o*-xylene, *N,N*-dimethyl formamide (DMF), methanol (MeOH), and anhydrous *N*-methyl-2-pyrrolidinone (NMP), were all purchased from Sigma-Aldrich and were of reagent-grade quality and used without further purification.

Ortho-hydroxy polyimide synthesis

For all the polyimides, the same synthesis route was followed. A three-necked flask equipped with a mechanical stirrer and gas inlet and outlet was charged with 20.0 mmol of the corresponding diamine and 20.0 ml of solvent (NMP). The solution was stirred at room temperature under argon atmosphere until the solid was completely dissolved. Then, the solution was cooled, by the use of an ice bath, to 0°C, and the required amounts of chlorotrimethyl silane and pyridine (1 mol/mol reactive group) and small amounts of DMAP (0.1 mol/mol pyridine) were added to the mixture. At that moment, the temperature was elevated to room temperature, and the solution was stirred for 15 min to ensure the formation of the silylated diamine. After this, the solution was again cooled down to 0°C, and the corresponding dianhydride (20.0 mmol) and additional solvent were added. The reaction mixture was stirred for 4 hours under these conditions, and then, the temperature was raised up to room temperature and left overnight for the formation of the poly(amic acid) in the solution. The viscosity of the solution significantly increased during this period.

o-Xylene (20 ml) as an azeotropic agent was then added to the solution, which was stirred vigorously and kept heated for 6 hours at 180°C to promote imidization. During this period, when the water was released by the ring-closure reaction, silanol and siloxane by-products were separated as a xylene azeotrope. After this time, leftover *o*-xylene was distilled out from the polymer solution. Subsequently, the mixture was cooled to room temperature and precipitated in distilled water. The pristine polymer thus obtained was repeatedly washed with water and ethanol and dried in a vacuum oven at 180°C for 24 hours.

Allyl-functionalized polymers

A three-necked flask, equipped with a condenser and gas inlet and outlet, was charged with 1 g of the corresponding polymer and 20 ml of DMF. After the polymer was completely dissolved, the adequate amount of K_2CO_3 (1 mol/1 mol of polymer) was added. Thirty minutes later, the allyl bromide (2 mol/1 mol of polymer) was added to the solution. Then, the temperature for the reaction was elevated to 60°C, and the solution was stirred for 12 hours under these conditions. After this time, the reaction broth was cooled to room temperature and precipitated in distilled water. The allyl-functionalized polymer was repeatedly washed with water and dried in a vacuum oven at 180°C for 24 hours.

Polymer film formation and thermal treatments

The casting of the polyimides was carried out from a 10 weight % filtered solution in NMP into a Teflon beaker with the leveled flat-bottom surface. The solvent was evaporated under nitrogen flow at 100°C, achieving the evaporation of the greater part of the solvent. Afterward, the isotropic polymer film was removed from the Teflon surface. Cast films were placed in a vacuum oven and dried overnight at 200°C in a vacuum oven equipped with a turbomolecular pumping unit to evaporate the remaining solvent. The defect-free and optically clean membranes were introduced in a muffle under nitrogen flow for treatment at higher temperatures (250°, 300°, 350°, 400°, and 450°C). The

heating rate was 5°C/min. The time at the corresponding target temperature was 1 hour, with the exception of the samples at 250°C, where the time of exposure to the target temperature of 250°C was 12 hours, and the sample at 450°C, where the time was 0.5 hours. Membranes at higher thermal treatments were treated at 250°C before the corresponding thermal protocol. This protocol was used to expose the prepared samples to the thermal treatment procedure similar to those reported in previous studies of TR polymers (36, 37).

Characterization of the polymers

Attenuated total internal reflectance (ATR)-FTIR experiments were conducted to verify the rearrangement process in the polymers. ATR-FTIR was performed at room temperature using a Bruker ALPHA FTIR spectrometer in a spectral range of 400 to 4000 cm^{-1} with a resolution of 2 cm^{-1} and an average of 32 scans. Thick membranes were directly measured.

Pristine and allyl-modified polyimides were completely soluble in DMSO. TR polymers (both pristine and allyl-containing) were completely insoluble in DMSO. The NMR study was accomplished with the AVANCE 500 spectrometer (Bruker GmbH), equipped with a 500-MHz magnet and a triple-resonance inverse probe. The liquid-phase experiments were carried out at room temperature with deuterated DMSO used as solvent and tetramethylsilane as internal standard. The NMR study confirmed the structure of the pristine polymer and the allylated product. The thermally treated polymers were insoluble in common solvents. For this reason, solid NMR was used to characterize the final structure of the polymers. The ^{13}C NMR of the allyl-functionalized polymer before and after thermal treatment at 350°C is shown in fig. S3.

DSC analysis was used to determine the T_g of polymers. DSC experiments were carried out with a calorimeter DSC 1 (Mettler Toledo), within the temperature measurement range from 50° to 450°C at a heating rate of 10 K/min. Measurements were accomplished in nitrogen atmosphere to prevent oxidation. Usually, the glass transition is determined in the second heating cycle to avoid the effect of sample preparation history rising, for example, from the remaining solvent traces. In our case, it is difficult to determine the T_g of the polymers synthesized in the course of the study because of the fact that the rearrangement process is happening normally at temperatures close to the T_g of the polymers. Thus, in this case, the collected data were extracted from the differences between the reversible and irreversible process.

TGA was used to determine the thermal stability and degree of conversion to PBO [as a function of the amount of CO_2 produced during the rearrangement observed by the IR spectrometer coupled with the TGA (17)] and the characteristic temperatures for the rearrangement: starting temperature, maximum rate of reaction, and final temperature. TGA experiments were carried out on the thermal analysis instrument NETZSCH TG 209 F1 Iris. The experiments were carried out at a temperature range from 25° to 800°C and at a heating rate of 5 K/min under a flux of 20 ml/min of argon. Disc-formed samples cut from films, with weights between 5 and 15 mg, were tested.

Additional TGA-FTIR was performed on a TGA-DSC2 Mettler Toledo coupled with an FT-IR spectrometer Nicolet iS50 Thermo Scientific in a spectral range of 400 to 4000 cm^{-1} , with a resolution of 4 cm^{-1} and an average of eight scans, to determine the volatile compounds produced during the thermal treatment. This experiment has confirmed the existence of only carbon dioxide as a volatile product of the thermal rearrangement process.

Mechanical properties of the thermally treated samples were tested using a Zwick 1478 universal testing machine (Zwick GmbH). The

measurements were performed at room temperature (24°C) at a traverse speed of 0.1 mm min⁻¹ for the Young modulus and 0.3 mm min⁻¹ as a test speed. To correctly assess the mechanical properties, six 4.5-mm-wide test strips were cut from each polymer sample and tested under the same conditions.

The permeability *P* was determined by using a permeator with constant volume variable pressure approach (known also as time lag method). The permeability coefficient measurements were carried out at 1000 mbar feed pressure and temperature of 30°C for H₂, He, N₂, O₂, CH₄ and CO₂. A sketch of the facility and the analysis method used have been described in previous studies (38).

SUPPLEMENTARY MATERIALS

Supplementary material for this article is available at <http://advances.sciencemag.org/cgi/content/full/2/7/e1501859/DC1>

fig. S1. IR spectra during the TGA as a function of the time (rate was 5°C/min) for pristine 6FDA-HAB polymer and allyl-functionalized 6FDA-HAB polymer.

fig. S2. FTIR for the allyl-functionalized 6FDA-HAB polymer at different temperatures of thermal treatment.

fig. S3. FTIR for the pristine and functionalized polymers derived from 6FDA-HAB before and after thermal rearrangement.

fig. S4. ¹H NMR for the polymer 6FDA-HAB.

fig. S5. ¹H NMR for the polymer 6FDA-HAB-allyl.

fig. S6. Solid-state ¹³C NMR for the polymer 6FDA-HAB-allyl after different thermal treatments.

fig. S7. Dynamic TGA for the pristine and functionalized polymers derived from 6FDA-BisAPAF, BTDA-BisAPAF, and PMDA-BisAPAF.

fig. S8. CO₂ solubility and diffusivity for the polymers studied in this work.

fig. S9. Robeson's trade-off for the separation CO₂/N₂ and O₂/N₂ gas pairs.

fig. S10. High feed pressure experiments for 6FDA-HAB-allyl thermally treated at 350°C.

table S1. Characteristic thermal points for the rearrangement and degradation temperature for the pristine and functionalized polymers derived from 6FDA-HAB.

table S2. Mechanical properties of the polymers under study.

table S3. Rearrangement properties for all the polymers synthesized in this work.

table S4. Results for the permeability of different pure gases and selectivity of different pairs of gases at 1 bar feed pressure and 30°C.

table S5. Physical properties of precursor allyl-functionalized polyimide (6FDA-HAB-allyl)- and allyl-TR-PBO-derived membranes.

REFERENCES AND NOTES

- R. Dawson, A. I. Cooper, D. J. Adams, Nanoporous organic polymer networks. *Prog. Polym. Sci.* **37**, 530–563 (2012).
- P. M. Budd, A. Butler, J. Selbie, K. Mahmood, N. B. McKeown, B. Ghanem, K. Msayib, D. Book, A. Walton, The potential of organic polymer-based hydrogen storage materials. *Phys. Chem. Chem. Phys.* **9**, 1802–1808 (2007).
- M. Carta, R. Malpass-Evans, M. Croad, Y. Rogan, J. C. Jansen, P. Bernardo, F. Bazzarelli, N. B. McKeown, An efficient polymer molecular sieve for membrane gas separations. *Science* **339**, 303–307 (2013).
- H. B. Park, C. H. Jung, Y. M. Lee, A. J. Hill, S. J. Pas, S. T. Mudie, E. Van Wagner, B. D. Freeman, D. J. Cookson, Polymers with cavities tuned for fast selective transport of small molecules and ions. *Science* **318**, 254–258 (2007).
- S. Kim, Y. M. Lee, Rigid and microporous polymers for gas separation membranes. *Prog. Polym. Sci.* **43**, 1–32 (2015).
- M. Calle, Y. Chan, H. J. Jo, Y. M. Lee, The relationship between the chemical structure and thermal conversion temperatures of thermally rearranged (TR) polymers. *Polymer* **53**, 2783–2791 (2012).
- S. H. Han, J. E. Lee, K.-J. Lee, H. B. Park, Y. M. Lee, Highly gas permeable and microporous polybenzimidazole membrane by thermal rearrangement. *J. Membr. Sci.* **357**, 143–151 (2010).
- S. H. Han, N. Misdan, S. Kim, C. M. Doherty, A. J. Hill, Y. M. Lee, Thermally rearranged (TR) polybenzoxazole: Effects of diverse imidization routes on physical properties and gas transport behaviors. *Macromolecules* **43**, 7657–7667 (2010).
- L. M. Robeson, The upper bound revisited. *J. Membr. Sci.* **320**, 390–400 (2008).
- C. P. Ribeiro, B. D. Freeman, D. S. Kalika, S. Kalakunnath, Aromatic polyimide and polybenzoxazole membranes for the fractionation of aromatic/aliphatic hydrocarbons by pervaporation. *J. Membr. Sci.* **390–391**, 182–193 (2012).
- N. Petzetakis, C. M. Doherty, A. W. Thornton, X. C. Chen, P. Cotanda, A. J. Hill, N. P. Balsara, Membranes with artificial free-volume for biofuel production. *Nat. Commun.* **6**, 7529 (2015).
- A. Hammami, N. Raymond, M. Armand, Lithium-ion batteries: Runaway risk of forming toxic compounds. *Nature* **424**, 635–636 (2003).
- Q. H. Wang, K. Kalantar-Zadeh, A. Kis, J. N. Coleman, M. S. Strano, Electronics and optoelectronics of two-dimensional transition metal dichalcogenides. *Nat. Nanotechnol.* **7**, 699–712 (2012).
- A. Corma, From microporous to mesoporous molecular sieve materials and their use in catalysis. *Chem. Rev.* **97**, 2373–2420 (1997).
- M. E. Davis, Ordered porous materials for emerging applications. *Nature* **417**, 813–821 (2002).
- D. F. Sanders, Z. P. Smith, R. Guo, L. M. Robeson, J. E. McGrath, D. R. Paul, B. D. Freeman, Energy-efficient polymeric gas separation membranes for a sustainable future: A review. *Polymer* **54**, 4729–4761 (2013).
- R. Guo, D. F. Sanders, Z. P. Smith, B. D. Freeman, D. R. Paul, J. E. McGrath, Synthesis and characterization of Thermally Rearranged (TR) polymers: Influence of *ortho*-positioned functional groups of polyimide precursors on TR process and gas transport properties. *J. Mater. Chem. A* **1**, 262–272 (2013).
- Z. P. Smith, K. Czenkusch, S. Wi, K. L. Gleason, G. Hernández, C. M. Doherty, K. Konstas, T. J. Bastow, C. Álvarez, A. J. Hill, A. E. Lozano, D. R. Paul, B. D. Freeman, Investigation of the chemical and morphological structure of thermally rearranged polymers. *Polymer* **55**, 6649–6657 (2014).
- L. Claisen, Rearrangement of phenol allyl ethers into *C*-allylphenols. *Chem. Ber.* **45**, 3157–3166 (1912).
- F. E. Ziegler, Stereo- and regiochemistry of the Claisen rearrangement: Applications to natural products synthesis. *Acc. Chem. Res.* **10**, 227–232 (1977).
- A. M. Martin Castro, Claisen rearrangement over the past nine decades. *Chem. Rev.* **104**, 2939–3002 (2004).
- H. Oie, A. Sudo, T. Endo, Synthesis of networked polymers by crosslinking reactions of polybenzoxazine bearing allyl group in the side chain. *J. Polym. Sci. Pol. Chem.* **51**, 2035–2039 (2013).
- S. Kotha, K. Mandal, A new protocol for benzoannulation by double Claisen rearrangement and ring-closing metathesis reactions as key steps. *Tetrahedron Lett.* **45**, 2585–2588 (2004).
- G. L. Tullos, J. M. Powers, S. J. Jeskey, L. J. Mathias, Thermal conversion of hydroxy-containing imides to benzoxazoles: Polymer and model compound study. *Macromolecules* **32**, 3598–3612 (1999).
- A. Kushwaha, M. E. Dose, Z. P. Smith, S. Luo, B. D. Freeman, R. Guo, Preparation and properties of polybenzoxazole-based gas separation membranes: A comparative study between thermal rearrangement (TR) of poly(hydroxyimide) and thermal cyclodehydration of poly(hydroxyamide). *Polymer* **78**, 81–93 (2015).
- S. Karan, Z. Jiang, A. G. Livingston, Sub-10 nm polyamide nanofilms with ultrafast solvent transport for molecular separation. *Science* **348**, 1347–1351 (2015).
- N. Du, H. B. Park, G. P. Robertson, M. M. Dal-Cin, T. Visser, L. Scoles, M. D. Guiver, Polymer nanosieve membranes for CO₂-capture applications. *Nat. Mater.* **10**, 372–375 (2011).
- D. F. Sanders, R. Guo, Z. P. Smith, K. A. Stevens, Q. Liu, J. E. McGrath, D. R. Paul, B. D. Freeman, Influence of polyimide precursor synthesis route and *ortho*-position functional group on thermally rearranged (TR) polymer properties: Pure gas permeability and selectivity. *J. Membr. Sci.* **463**, 73–81 (2014).
- H. J. Jo, C. Y. Soo, G. Dong, Y. S. Do, H. H. Wang, M. J. Lee, J. R. Quay, M. K. Murphy, Y. M. Lee, Thermally rearranged poly (benzoxazole-co-imide) membranes with superior mechanical strength for gas separation obtained by tuning chain rigidity. *Macromolecules* **48**, 2194–2202 (2015).
- Y. Zhuang, J. G. Seong, W. H. Lee, Y. S. Do, M. J. Lee, G. Wang, M. D. Guiver, Y. M. Lee, Mechanically tough, thermally rearranged (TR) random/block poly(benzoxazole-co-imide) gas separation membranes. *Macromolecules* **48**, 5286–5299 (2015).
- W. J. Koros, R. Mahajan, Pushing the limits on possibilities for large scale gas separation: Which strategies? *J. Membr. Sci.* **175**, 181–196 (2000).
- M. Rungta, L. Xu, W. J. Koros, Structure–performance characterization for carbon molecular sieve membranes using molecular scale gas probes. *Carbon* **85**, 429–442 (2015).
- Y. Jiang, F. T. Willmore, D. Sanders, Z. P. Smith, C. P. Ribeiro, C. M. Doherty, A. Thornton, A. J. Hill, B. D. Freeman, I. C. Sanchez, Cavity size, sorption and transport characteristics of thermally rearranged (TR) polymers. *Polymer* **52**, 2244–2254 (2011).
- R. L. Burns, W. J. Koros, Structure–property relationships for poly(pyrrolone-imide) gas separation membranes. *Macromolecules* **36**, 2374–2381 (2003).
- J. N. Barsema, S. D. Klijnstra, J. H. Balster, N. F. A. van der Vegt, G. H. Koops, M. Wessling, Intermediate polymer to carbon gas separation membranes based on Matrimid Pl. *J. Membr. Sci.* **238**, 93–102 (2004).

36. B. Comesaña-Gándara, M. Calle, H. J. Jo, A. Hernández, J. G. de la Campa, J. de Abajo, A. E. Lozano, Y. M. Lee, Thermally rearranged polybenzoxazoles membranes with biphenyl moieties: Monomer isomeric effect. *J. Membr. Sci.* **450**, 369–379 (2014).
37. D. F. Sanders, R. Guo, Z. P. Smith, Q. Liu, K. A. Stevens, J. E. McGrath, D. R. Paul, B. D. Freeman, Influence of polyimide precursor synthesis route and *ortho*-position functional group on thermally rearranged (TR) polymer properties: Conversion and free volume. *Polymer* **55**, 1636–1647 (2014).
38. A. M. Shishatskii, Y. P. Yampol'skii, K.-V. Peinemann, Effects of film thickness on density and gas permeation parameters of glassy polymers. *J. Membr. Sci.* **112**, 275–285 (1996).

Acknowledgments: We would like to thank S. Neuman, T. Emmeler, K. Buhr, J. Grünauer, C. Otto, and P. Georgopoulos for technical support. **Funding:** This work was financially supported by Helmholtz Association of German Research Centers through the Helmholtz Portfolio MEM-BRAIN. **Author contributions:** A.T.: experimental design, synthesis, gas permeation experiments, characterization

experiments, and manuscript writing; S.R.: experimental design, synthesis, and characterization experiments; S.S.: gas permeation experiments, industrial application input, and manuscript writing; V.F.: NMR analysis and supervision; V.A.: direction and supervision, and manuscript writing. All the authors contributed to the data analysis, results discussion, and revision. **Competing interests:** The authors declare that they have no competing interests. **Data and materials availability:** All data needed to evaluate the conclusions in the paper are present in the paper and/or the Supplementary Materials. Additional data related to this paper may be requested from the authors.

Submitted 18 December 2015

Accepted 29 June 2016

Published 29 July 2016

10.1126/sciadv.1501859

Citation: A. Tena, S. Rangou, S. Shishatskiy, V. Filiz, V. Abetz, Claisen thermally rearranged (CTR) polymers. *Sci. Adv.* **2**, e1501859 (2016).

Claisen thermally rearranged (CTR) polymers

Alberto Tena, Sofia Rangou, Sergey Shishatskiy, Volkan Filiz and Volker Abetz

Sci Adv 2 (7), e1501859.

DOI: 10.1126/sciadv.1501859

ARTICLE TOOLS

<http://advances.sciencemag.org/content/2/7/e1501859>

SUPPLEMENTARY MATERIALS

<http://advances.sciencemag.org/content/suppl/2016/07/25/2.7.e1501859.DC1>

REFERENCES

This article cites 38 articles, 3 of which you can access for free
<http://advances.sciencemag.org/content/2/7/e1501859#BIBL>

PERMISSIONS

<http://www.sciencemag.org/help/reprints-and-permissions>

Use of this article is subject to the [Terms of Service](#)

Science Advances (ISSN 2375-2548) is published by the American Association for the Advancement of Science, 1200 New York Avenue NW, Washington, DC 20005. The title *Science Advances* is a registered trademark of AAAS.

Copyright © 2016, The Authors